Performance Trade-off Analysis of Co-design of Radar and Phase Modulated Communication Signals in Frequency Hopping MIMO Systems

Indu Priya Eedara and Moeness G. Amin

Center for Advanced Communications, Villanova University, Villanova, PA, 19085, USA
E-mail: {ieedara; moeness.amin}@villanova.edu

ABSTRACT

We present a dual-function radar communication (DFRC) system in which phase modulated information symbols are embedded in the multiple-input multiple-output (MIMO) frequency hopping (FH) radar sub-pulses in fast-time. The communications is considered as the secondary function of the proposed dual-function radar communication (DFRC) systems. We use differential phase shift keying (DPSK) and continuous phase modulation (CPM). These modulations preserve the continuous phase between the FH sub-pulses, unlike phase shift keying (PSK) modulated symbols. The performance of FH/DPSK and FH/CPM systems is compared with that of the FH/PSK system in terms of range sidelobe levels (RSL) and power spectral density (PSD). It is shown that the proposed DFRC systems exhibit better spectral containment and lower spectral sidelobe levels. The communication data rates for the proposed system are derived, and to assume relatively high values.

Keywords: MIMO, FH, Dual-Function, Radar-Commuications, CPM, DPSK, PSK

1. INTRODUCTION

Radar and Communications co-existence has been proposed as a solution for spectral congestion caused by increased demands of wireless industry.[1–4] As a solution to this problem, dual-function radar-communication (DFRC) systems were proposed in.[5,6] The communications is treated as secondary to the primary radar function. The DFRC systems make full use of the radar resources such as high quality hardware and high transmit power. For the DFRC system, information embedding into the emission of single-input multiple-output (SIMO) radar can be achieved using waveform diversity, sidelobe control, or time modulated array. Information embedding into the emission of multiple-input multiple-output (MIMO) radar was considered in.[7,8] Alternative names used in the literature for the DFRC system are RF convergence, Intentional Modulation on a Pulse and Co-Radar.[9,10] Frequency hopping (FH) waveforms are attractive for radar and communications since they have constant modulus and are easy to generate.[11] In the DFRC system considered, the phase modulated communication symbols are embedded in each hop of the FH waveforms. Modulation of FH sub-pulses with phase shift keying (PSK) symbols was proposed and analyzed in.[6,12] The phase rotation resulting from the PSK symbol embedding disrupts the continuous phase between the FH sub-pulses. This causes an adverse effect of increased spectral side lobes and spectral leakage into adjacent frequency bands.[13] To overcome this shortcoming, we propose the modulation of FH radar sub-pulses with differential phase shift keying (DPSK) and continuous phase modulation (CPM) signals.

DPSK and CPM modulations are generally the preferred methods to contain spectral leakage as both maintain constant modulus. Although the DPSK modulation preserves the continuous phase between the FH sub-pulses, the first derivative of the phase is not continuous and hence the spectral spreading still exists. The first derivative of the phase of CPM signals is continuous allowing the CPM signals to offer better spectral containment compared to PSK and DPSK modulations. Therefore, we consider herein the CPM information embedding for FH radar waveforms.

In this paper, we present three types of phase modulated FH DFRC systems, namely, FH/PSK, FH/DPSK, FH/CPM. We compare the performance of these systems by examining the range sidelobe levels (RSL) and power spectral density (PSD) pre- and post- symbol embedding. The proposed DFRC systems offer reduction in

This work is supported by NSF award #AST- 1547420.

the RSL, an improvement in the spectral sidelobe levels. This, in turn, permits higher FH coefficient recurrence, thereby increasing the achievable communication data rate.
The paper is organized as follows. The details of the DFRC system design, the FH waveforms, PSK, DPSK and CPM symbol embedding are presented in Section 2. Bandwidth requirements and MIMO radar receive signal model is presented in Section 3, analysis of the DFRC waveforms is presented in Section 4. Simulations are provided in Section 5, and the conclusions are drawn in Section 6.

2. MIMO DFRC SYSTEM DESIGN

We consider a system equipped with a common dual-function transmit platform. The common transmit array comprises M_T omni-directional transmit antennas. The MIMO radar co-located receive array has N antennas arranged in a linear shape. For a MIMO system, the radar transmit waveforms $\beta_m(t)$, $m = 1 \dots M_T$, should satisfy the orthogonality condition, i.e.,

$$\int_{T_p} \beta_m(t)\beta^*_{m'}(t+\tau)e^{j2\pi\nu t}dt = \begin{cases} \delta(\tau)\delta(\nu), & m = m', \\ 0, & \text{otherwise} \end{cases} \tag{1}$$

where, t is the fast-time index, T_p is the pulse duration, $(\cdot)^*$ denotes the conjugate of a complex number, τ and ν denote time delay and Doppler shift, respectively and $\delta(\cdot)$ is the Kronecker delta function. It is difficult to synthesize waveforms which satisfy the ideal orthogonality condition (1). Practical waveforms, which can be efficiently synthesized, are discussed in,[7] and references therein.

2.1 Frequency-Hopping Waveforms

FH waveforms meet the MIMO radar requirements, like high transmit power efficiency, high range and Doppler resolution properties.[11,14] The FH waveform transmitted from m^{th} antenna can be expressed as,

$$\beta_m(t) = \sum_{q=1}^{Q} e^{j2\pi c_{m,q}\Delta_f t}u(t - q\Delta_t), \tag{2}$$

where $c_{m,q},\ m = 1, \dots, M_T,\ q = 1, \dots, Q$ denote the FH coefficients, Q is the number of sub-pulses derived from K available frequencies ($K \geq Q$), Δ_f and Δ_t are the frequency step and the sub-pulse duration, respectively, and

$$u(t) \triangleq \begin{cases} 1, & 0 < t < \Delta_t, \\ 0, & \text{otherwise.} \end{cases} \tag{3}$$

is a rectangular pulse of duration Δ_t. Equation (2) states that each FH waveform contains Q sub-pulses, i.e., the radar pulse duration $T_p = Q\Delta_t$. It is also assumed that $\Delta_t\Delta_f$ is an integer. In this paper, we choose $\Delta_t\Delta_f = 1$.[11] For symbol detection, it is important for the communication function that we choose

$$c_{m,q} \neq c_{m',q}, \qquad \forall q, m \neq, m'. \tag{4}$$

2.2 PSK Symbol Embedding

Let $\{\Omega_{(m,q)} \in \mathbb{D}_{\text{PSK}}\},\ m = 1, \dots, M_T,\ q = 1, \dots, Q$ be a set of PSK symbols that need to be embedded into the MIMO radar pulse, where the PSK dictionary of size J is defined as $\mathbb{D}_{\text{PSK}} = \left\{0, \frac{2\pi}{J}, \dots, \frac{(J-1)2\pi}{J}\right\}$. Each PSK symbol represents $N_{\text{bit}} = \log_2 J$ bits. The PSK-modulated FH radar waveforms can be expressed as[6]

$$\psi_m^{PSK}(t) = \sum_{q=1}^{Q} e^{j\Omega_{(m,q)}}h_{m,q}(t)u(t - q\Delta_t), \tag{5}$$

where $h_{m,q}(t) \triangleq e^{j2\pi c_{m,q}\Delta_f t}$ is the FH signal associated with the m^{th} antenna.

2.3 DPSK Symbol Embedding

We discuss embedding in FH sub-pulses with DPSK phase modulated waveforms. We implement the DPSK waveform structure presented in.[15] For high power applications, radar codes must be constant modulus so as to maximize the energy on target. Therefore, mostly all codes are designed with the implicit assumption that each code value is modulated onto a square-shaped chip. There are Q sub-pulses available in the FH radar pulse, each sub-pulse is embedded with an information symbol. The information symbol is represented by a phase, $\Omega_{(m,q)}$. The phase sequence can be expressed using a sequence of rectangular chips as,

$$s_m(t) = \sum_{q=1}^{Q} e^{j\Omega_{(m,q)}} u(t - q\Delta_t), \tag{6}$$

where, $\Omega_{(m,q)}$ is the phase value of the q^{th} sub-pulse from m^{th} antenna. The DPSK modulation of the code sequence in (6) for m^{th} transmit antenna is given by,

$$\zeta_m(t) = s_m\left(t - \Delta_t/2\right)\left|\cos\left(\frac{\pi t}{\Delta_t}\right)\right| - j s_m(t)\left|\sin\left(\frac{\pi t}{\Delta_t}\right)\right|. \tag{7}$$

The above equation infers that the phase of $\zeta_m(t)$ is continuous across the sub-pulse boundaries $q\Delta_t$. For the sake of simplicity, and for all practical purposes, we assume $J = 2$, i.e., $\Omega_{(m,q)} \in (0, \pi)$. The DPSK modulated FH MIMO radar waveform from m^{th} antenna can be represented as,

$$\psi_m^{DPSK}(t) = \beta_m(t).\zeta_m(t). \tag{8}$$

2.4 CPM Symbol Embedding

The continuous phase modulation signals preserves the phase continuity between the successive symbols. The constant envelope feature translates to robustness against the distortion introduced by non-linear components in the transmitter while the continuous phase feature of CPM signals leads to high spectral efficiency.[16]
The complex baseband CPM signal for m^{th} transmit antenna can be expressed as

$$s_{m,\phi}(t; \boldsymbol{\alpha}) = e^{j\phi(t;\boldsymbol{\alpha})}. \tag{9}$$

The phase can be defined as a pulse train[16] of the form,

$$\phi(t; \boldsymbol{\alpha}) = 2\pi \sum_i h_i \alpha_i b(t - i\Delta_t), \tag{10}$$

where α_i is an M-ary symbol which can be selected from the alphabet sequence $\{\pm 1, \pm 3, \ldots, \pm(M-1)\}$, h_i is the sequence of modulation indices used during the i^{th} symbol interval which are selected in a cyclic manner and h_i is a rational number. $b(t)$ is the phase pulse which is the time-integral of a frequency pulse $g(t)$, i.e.,

$$b(t) = \int_0^t g(p)dp. \tag{11}$$

If $g(t) = 0$ for $t > \Delta_t$, the signal is called full-response CPM. If $g(t) \neq 0$ for $t > \Delta_t$, then that signal is called a partial-response CPM. Rectangular and raised cosine frequency pulse shapes have been defined in.[17] Partial-response pulses extend over a duration of $L\Delta_t$, where, L is a positive integer. When $L = 1$, the signal is called a full-response CPM. The rectangular and raised cosine pulses for $L = 1$ and 3 and their integrals are shown in Figure. 1. The general expressions for the rectangular and raised cosine frequency pulses, $g(t)$ can be expressed as,

$$\text{LREC} \qquad g(t) = \begin{cases} \frac{1}{2L\Delta_t}, & 0 \leq t \leq L\Delta_t, \\ 0, & \text{otherwise.} \end{cases}$$

$$\text{LRC} \qquad g(t) = \begin{cases} \frac{1}{2L\Delta_t}\left(1 - cos\left(\frac{2\pi t}{L\Delta_t}\right)\right), & 0 \leq t \leq L\Delta_t, \\ 0, & \text{otherwise.} \end{cases}$$

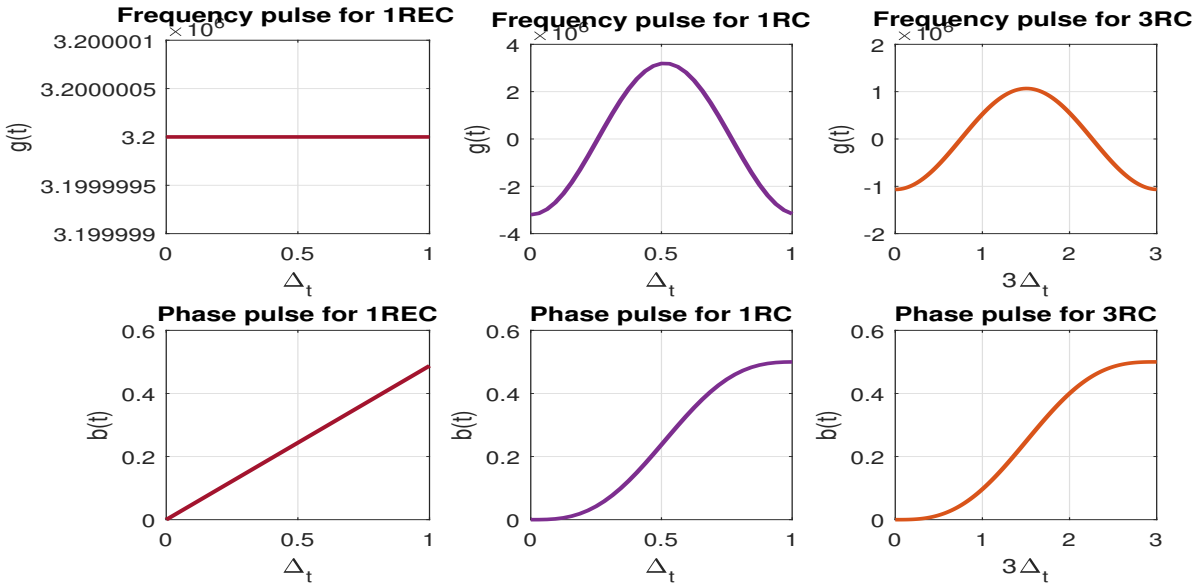

Figure 1: Rectangular and raised cosine frequency pulses and their respective phase pulses for duration $L\Delta_t$, L=1 and 3.

Accordingly, the CPM signal can be defined by the parameters M, $g(t)$, L and h_i. If the modulation index varies from symbol to symbol in a cyclic manner, it is referred to as multi-h CPM signal. The general phase expression of the CPM signal with memory during q^{th} sub-pulse can be expressed as,

$$\phi(t;\boldsymbol{\alpha}) = 2\pi \sum_{i=q-L+1}^{q} h_i \alpha_i b(t - i\Delta_t) + \pi \sum_{i=0}^{q-L} h_i \alpha_i. \tag{12}$$

During q^{th} sub-pulse, the symbol $\boldsymbol{\alpha}$ assumes the values, $\boldsymbol{\alpha} = \{\alpha_{q-L+1}, \ldots, \alpha_{q-1}, \alpha_q\}$. The phase values for each sub-pulse duration are computed using (12). Finally, the CPM modulated FH MIMO radar waveforms from m^{th} transmit antenna is given as,

$$\psi_m^{CPM}(t) = \beta_m(t).s_{m,\phi}(t;\boldsymbol{\alpha}). \tag{13}$$

3. BANDWIDTH REQUIREMENTS AND RECEIVE SIGNAL MODEL

3.1 Bandwidth Requirements

Let B denote the bandwidth assigned to the DFRC system. To insure that the spectral contents of the orthogonal FH waveforms are confined to the available bandwidth, the FH code, $c_{m,q}$ should be selected from the set of integers $\{0, 1, \ldots, K-1\}$, where $K \approx \frac{B}{\Delta_f}$,

$$B_{\text{eff}} \approx (K-1)\Delta_f + \frac{1}{\Delta_t}, \tag{14}$$

and the condition $B_{\text{eff}} \leq B$ is satisfied. The time-bandwidth product of the DFRC system is given as,

$$BT_p = \left((K-1)\Delta_f + \frac{1}{\Delta_t}\right) Q\Delta_t = KQ. \tag{15}$$

3.2 MIMO Radar Receive Signal Model

Assume that the signals reflected by L targets impinge on the MIMO radar receiver from directions θ_ℓ, $\ell = 1, \ldots, L$. The $N \times 1$ complex-valued vector of the received baseband signals can be represented as,

$$\mathbf{x}(t,n) = \sum_{\ell=1}^{L} \eta_\ell(n) \left[\mathbf{a}^T(\theta_\ell)\boldsymbol{\psi}(t,n)\right] \mathbf{b}(\theta_\ell) + \mathbf{z}(t,n), \tag{16}$$

where n denotes the slow-time index, i.e., pulse number, $\eta_\ell(n)$ is the reflection coefficient associated with the ℓ^{th} target during the n^{th} pulse, θ_ℓ is the spatial angle of the ℓ^{th} target, $\mathbf{a}(\theta_\ell)$ and $\mathbf{b}(\theta_\ell)$ are the steering vectors of the transmit and receive arrays towards the direction θ_ℓ, respectively, $(\cdot)^T$ stands for the transpose, $\boldsymbol{\psi}(t,n) \in \{\boldsymbol{\psi}^{PSK}(t,n), \boldsymbol{\psi}^{DPSK}(t,n), \boldsymbol{\psi}^{CPM}(t,n)\}$ and $\boldsymbol{\psi}(t,n) \triangleq [\psi_1(t,n), \ldots, \psi_{M_T}(t,n)]^T$ is the $M_T \times 1$ complex vector of phase modulated waveforms. $\mathbf{z}(t,n)$ is an $N \times 1$ vector of zero-mean white Gaussian noise with variance σ_z^2. Matched filtering (16) to the transmitted orthogonal waveforms yields the $M_T N \times 1$ data vector,

$$\begin{aligned}\mathbf{y}(n) &= \text{vec}\left(\int_{T_p} \mathbf{x}(t,n)\boldsymbol{\psi}(t,n)^H(t)\,dt\right) \\ &= \sum_{\ell=1}^{L} \eta_\ell(n)\left[\mathbf{a}(\theta_\ell) \otimes \mathbf{b}(\theta_\ell)\right] + \tilde{\mathbf{z}}(n),\end{aligned} \tag{17}$$

where $\text{vec}(\cdot)$ denotes the vectorization operator that stacks the columns of a matrix into one long column vector, $\otimes$ denotes the Kronecker product, $(\cdot)^H$ stands for the Hermitian transpose, $\tilde{\mathbf{z}}(n)$ is $M_T N \times 1$ vector of additive noise at the output of the matched-filters with zero-mean and co-variance $\sigma_z^2 \mathbf{I}_{M_T N}$, and $\mathbf{I}_{M_T}$ is the identity matrix of size $M_T \times M_T$.

Consider a single-antenna communication receiver located at in the spatial direction θ_c with respect to the MIMO radar. The signal at the output of the communication receiver is,

$$r(t,n) = \alpha_{\text{ch}} \mathbf{a}^T(\theta_c)\boldsymbol{\psi}(t,n) + w(t,n), \tag{18}$$

where α_{ch} is the channel coefficient which summarizes the propagation environment between the transmit array and the communication receiver and $w(t,n)$ represents the additive white Gaussian noise with zero mean and variance σ_w^2.

Assume that time and phase synchronizations between the MIMO radar and the communication receiver are achieved and the transmitted FH sequence is known at the receiver. Matched filtering $r(t,n)$ to the FH sub-pulses yields the communication signal,

$$y_{m,q}(n) = \int_{\Delta_t} r(t,n) h_{m,q}^*(t) u(t - q\Delta_t - nT_0)dt, \tag{19}$$

where, $h_{m,q}(t) \triangleq e^{j2\pi c_{m,q}\Delta_f t}$ is the FH signal associated with the m^{th} antenna during the q^{th} sub-pulse. Then, the communication symbols can be demodulated using the demodulators for the type of phase modulation used.

4. ANALYSIS OF THE PROPOSED DFRC WAVEFORMS

In this section, we analyze the range sidelobes performance, power spectral density and the communication data rate that can be achieved by the proposed phase modulated FH MIMO radar waveforms.

4.1 Range sidelobe performance

4.1.1 Without Symbol Embedding

Without loss of generality, we consider the case of a DFRC system with uniform linear arrays. The inter-element spacings associated with the transmit and receive arrays are denoted as d_T and d_R, respectively. The spatial

frequency of a target located in direction θ is defined as $f = 2\pi d_R sin(\theta)$, where d_R is measured in wavelength. Adopting the AF definition from,[14] the AF expression for the MIMO radar can be written as,

$$|\chi(\tau, \nu, f, f')| \triangleq \left| \sum_{m=1}^{M_T} \sum_{m'=1}^{M_T} \chi_{m,m'}(\tau, \nu) e^{j2\pi(fm - f'm')\gamma} \right|, \tag{20}$$

where, τ, ν, f, f' denote time delay, Doppler shift, spatial frequency, and spatial frequency shift, respectively, and $\gamma \triangleq d_T/d_R$. For zero Doppler shift ($\nu = 0$) and $f = f'$, (20) can be re-written as,

$$|\chi(\tau, 0)| \triangleq \left| \sum_{m=1}^{M_T} \sum_{m'=1}^{M_T} \chi_{m,m'}(\tau, 0) \right|. \tag{21}$$

We can compute the range sidelobe response from[14] for the FH MIMO radar waveforms as,

$$\Gamma_{\text{rad}}(\tau) = \chi_{m,m'}(\tau, 0) \triangleq \int_0^{T_p} \beta_m(t) \beta^*_{m'}(t + \tau), \tag{22}$$

where, $\Gamma_{\text{rad}}(\tau)$ is the correlation function between the FH waveforms from antennas m and m'. At delays $\tau = c\Delta_t$, $c = 0, 1, \ldots, Q-1$, due to the re-use of frequencies in the FH sub-pulses, the FH MIMO radar system exhibits high range sidelobes.[18]

4.1.2 With Symbol Embedding

The range sidelobe levels for the DFRC system with symbol embedding can be computed as,

$$\Gamma_{\text{DF}}(\tau) = \chi_{m,m'}(\tau, 0) \triangleq \int_0^{T_p} \psi_m(t) \psi^*_{m'}(t + \tau). \tag{23}$$

At $\tau = c\Delta_t$, due to the randomness of the phase values, the terms inside the summations of (20) cancel each other, resulting in significant reduction of the range sidelobe levels. As a result, a large number of DFRC waveforms can be synthesized with frequency re-use across the sub-pulses.

A. PSK and DPSK

The phase values for PSK and DPSK symbols are selected from $\Omega_{(m,q)} \in \mathbb{D} = \left\{0, \frac{2\pi}{J}, \ldots, \frac{(J-1)2\pi}{J}\right\}$. Therefore, when there is re-use of frequencies at $\tau = c\Delta_t$, the FH/PSK and FH/DPSK systems result in lower values of RSL. When the values of $\Omega_{(m,q)} = 0$, both the DFRC systems revert back to the FH MIMO radar system without embedding.

B. CPM

When $\tau = c\Delta_t$, the RSL of the FH/CPM system depends on the modulation index and the M-ary alphabet size. When $h_i = 0$ or $h_i \approx 0$, the FH/CPM waveforms are close to the FH MIMO radar waveforms without embedding. As the alphabet size, h_i increases, using multi-h CPM, the degree of randomness in the phase values increases and hence the reduction in RSL.

4.2 Power Spectral Density (PSD)

The effect of symbol embedding on the PSD of the FH MIMO radar system is presented in this section.

4.2.1 DPSK

Unlike PSK symbol embedding, the DPSK modulation presented in this paper results in smooth transitions between the FH MIMO sub-pulses. Therefore, the DPSK symbol embedding leads to lower spectral sidelobes compared to that of PSK embedding. Since the first derivative of the phase for the DPSK modulation is not continuous, this can still cause spectral broadening.[19] This adverse effect can be avoided by setting few of the phase values used to define the symbols at the high and low frequencies of the spectrum, $\Omega_{m,q} = 0°$.

4.2.2 CPM

CPM has better spectral efficiency compared to DPSK and PSK modulations. The spectral characteristics of the CPM signal depend on the design parameters h_i, shape of the frequency pulse, $g(t)$ and L. Small values of h_i result in CPM signals with relatively small bandwidth occupancy, while large values of h_i result in signals with large bandwidth occupancy.[17] Use of smooth pulses such as raised cosine pulses also result in smooth transition between the symbols. When $L > 1$, each pulse extends over multiple symbols duration. As a result, the pulse $b(t)$ becomes more smoother and hence the better spectral efficiency.[20,21] Accordingly, the use of multi-h, partial-response CPM with smooth pulse shapes is preferred to have good spectral characteristics. But, the demodulator complexity at the communication receiver increases when partial-response CPM is used. We present CPM modulations with different design parameters in Sec. 5, to demonstrate the effect of symbol embedding on PSD of the FH MIMO radar.

4.3 Data Rate

The achievable communication data rate (DR) for the DFRC system can be readily shown[6] to be proportional to the pulse repetition frequency, the number of transmit elements, the length of the FH code, and the size of the symbol constellation. Here, the antennas, M_T can take a maximum of K frequency values. Thus, the data rate becomes, $DR = PRF.K.Q.log_2(M)$ for FH/CPM, and $DR = PRF.K.Q.log_2(J)$ for FH/PSK and FH/DPSK systems. By implementing the condition,

$$c_{m,q} \neq c_{m',q'}, \qquad m \neq m' \quad \& \quad q \neq q' \tag{24}$$

there will be minimum correlation between the FH sub-pulses and hence the communication symbol embedding does not show pronounced effect on RSL. But, using (24), reduces the number of hops and antennas that can be implemented to $M_T Q = K$. The maximum data rate in this case becomes $DR = PRF.K.log_2(M)$ for FH/CPM and $DR = PRF.K.log_2(J)$ for FH/PSK and FH/DPSK systems. This is less than the data rate that can be achieved with re-use of coefficients in the FH code matrix. Therefore, with minimal effort in designing the code matrix, we can utilize information symbol embedding to improve the data rate of the system.

5. SIMULATIONS

We consider a MIMO radar system operating at X-band with carrier frequency $f_c = 8.2$ GHz and bandwidth 105 MHz. The sampling frequency is taken as the Nyquist rate, i.e., $f_s = 2 \times 1.5 \times 10^8$ sample/sec. The pulse repetition interval (PRI) is $T_0 = 10\ \mu s$, i.e., the pulse repetition frequency (PRF) is 100 KHz. The transmit array is considered to be a ULA comprising $M_T = 16$ omni-directional transmit antennas spaced half a wavelength apart. We generate a set of 16 FH waveforms. The parameter $K = 16$ is chosen such that the FH step is $\Delta_f = 6.4$ MHz. The FH code length $Q = 16$ is assumed and the FH interval duration $\Delta_t = 0.156\ \mu s$ is used. The 16×16 FH code is generated randomly from the set $\{1, 2, \ldots, K\}$, where $K = 16$. The values of $J = 2$, $M = 4$ and $L = 1, 3$, and the same values of FH code are used for all the DFRC systems presented in this paper.

Example 1: RSL

The RSL response for FH/PSK and FH/DPSK systems is shown in Figure. 2. It can be noticed that, at $\tau = c\Delta_t$, the randomness of the PSK and DPSK symbols helps in RSL reductions. It can also be observed that the maximum value of RSL of the FH/PSK and FH/DPSK systems does not exceed the upper bound of RSL of the FH system without embedding. With CPM symbol embedding, the phase is continuous between the sub-pulses, and the phase trees for different frequency pulse shapes are shown in Figure. 3 for $M = 4$ and $h_i = 4/16$. The phase tree for a rectangular pulse shape shown in Figure. 3 (a) exhibits sharp phase transitions maintaining the continuous phase between symbols. Phase trees for raised cosine pulses with $L = 1, 3$ respectively, are shown in Figure. 3 (b), (c). It is shown that use of raised cosine pulse results in smoother phase transitions between the symbol intervals and this becomes even smoother when 3RC CPM is used.

The RSL of the FH/CPM system for the parameters 3RC, 1RC and 1REC are presented in Figure. 4 and are compared with FH MIMO radar system without symbol embedding. It is shown in Figure. 4 (a) (b), for $h_i = 1/32, 1/16$ that, when $h_i \approx 0$, the RSL of the FH/CPM system are similar to the FH MIMO radar system without embedding. It is shown in Figure. 4 (c) and (d), for $h_i = 1/4, 1/2$ that the RSL decreases with increased

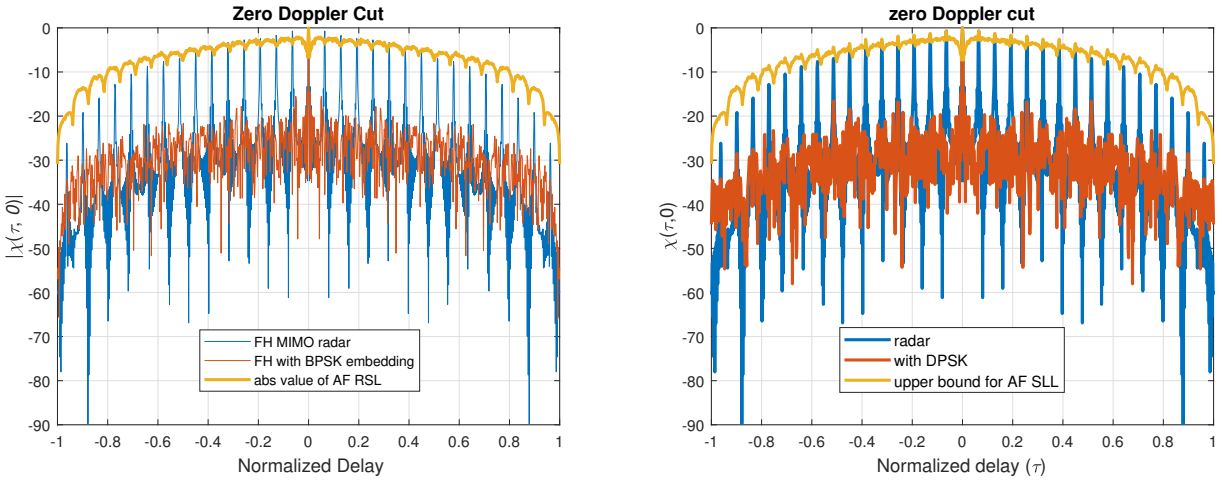

(a) PSK symbol embedding (b) DPSK symbol embedding

Figure 2: RSL of FH/PSK, FH/DPSK and FH MIMO radar system without embedding.

value of h_i. It can also be observed from Figure. 4 (e) and (f) that use of multi-h CPM shows improvement in the RSL compared to single-h CPM in FH/CPM MIMO DFRC systems.

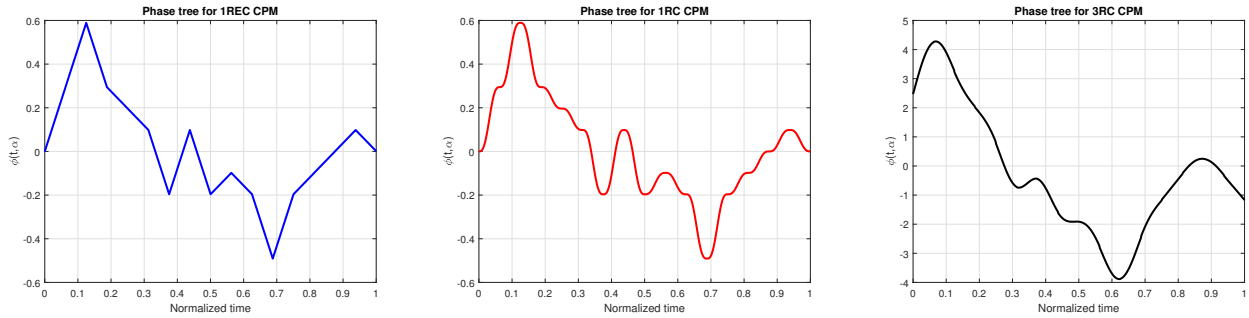

(a) Phase tree for 1REC (b) Phase tree for 1RC (c) Phase tree for 3RC

Figure 3: Phase trees for 4-ary CPM signals with different pulse shapes

Example 2: PSD

The PSD of the FH/CPM DFRC system for the parameters presented in Figure. 4 is shown in Figure. 5. It can be observed from Figure. 5 (a), (b) that when $h_i \approx 0$, the PSD of the FH/CPM DFRC system is similar to the FH radar system without embedding. But, as h_i increases, in Figure. 5 (c)-(f), there is spectral broadening and the spectral sidelobes roll-off. The spectral broadening is more pronounced with the use of 1RC and 1REC CPM compared to 3RC CPM. Figure. 5 (f) shows the PSD of 4- ary, 3RC CPM with $h_1 = 4/16, h_2 = 5/16$, a configuration which is extensively used in Aeronautical Telemetry. This configuration has lower spectral sidelobes and also shows no spectral broadening.

Example 3: Comparison between FH MIMO radar systems with and without symbol embedding

Figure. 6 shows the RSL response and PSD of FH/PSK, FH/DPSK, FH/CPM MIMO DFRC systems and FH MIMO system without embedding. It is shown in Figure. 6 (a) that all the FH MIMO DFRC systems presented in this paper exhibit better RSL response compared to FH MIMO radar system without embedding. For the same FH code, FH/CPM system has better RSL response compared to FH/PSK and FH/DPSK DFRC systems. From Figure. 6 (b), it is evident that the FH/DPSK system exhibits low spectral sidelobes, but there is spectral broadening and the FH/PSK system shows high spectral sidelobe levels. The FH/CPM system shows better

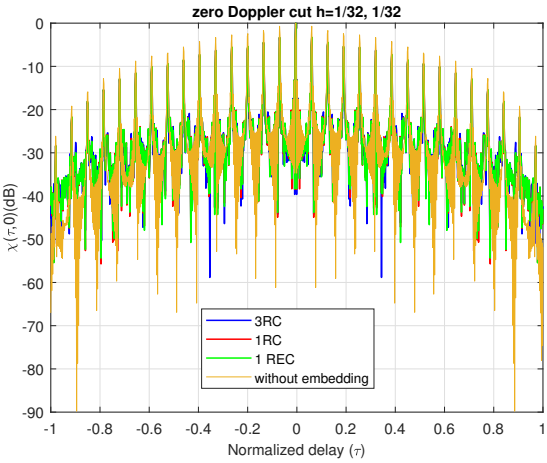

(a) RSL for h=1/32

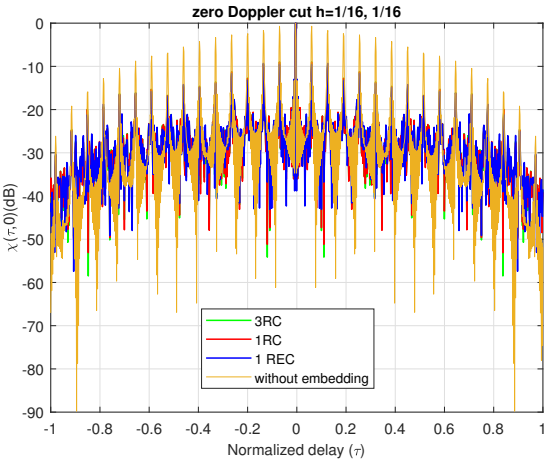

(b) RSL for h=1/16

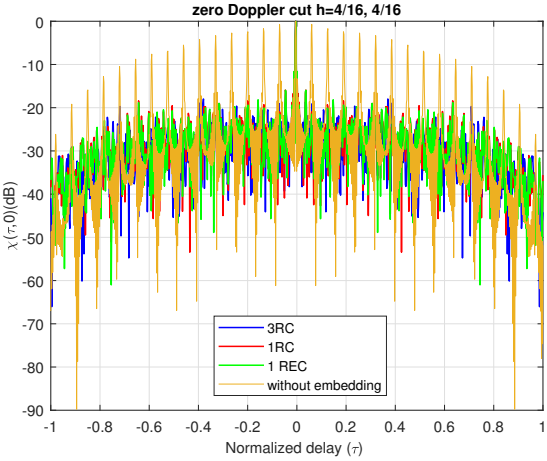

(c) RSL for h=1/4

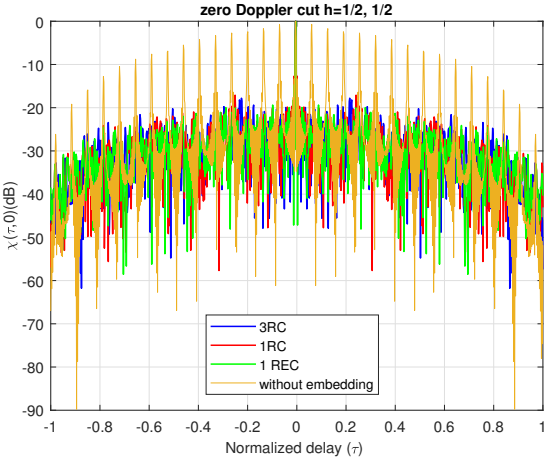

(d) RSL for h=1/2

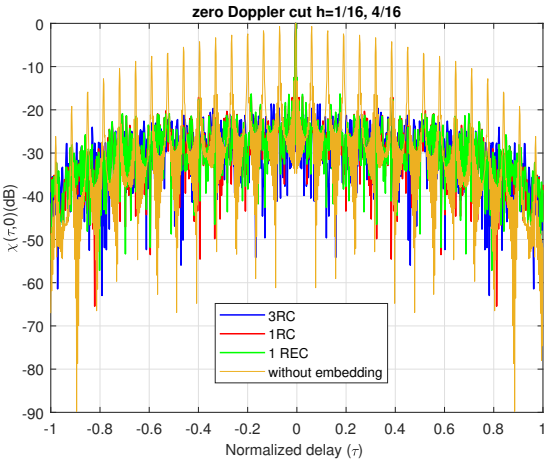

(e) RSL for $h_1 = 1/16$ and $h_2 = 4/16$

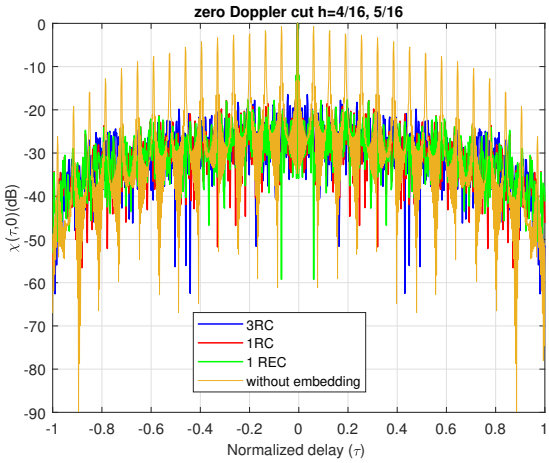

(f) RSL for $h_1 = 4/16$ and $h_2 = 5/16$ ARTM

Figure 4: RSL for 4-ary CPM with different pulse shapes and modulation indices

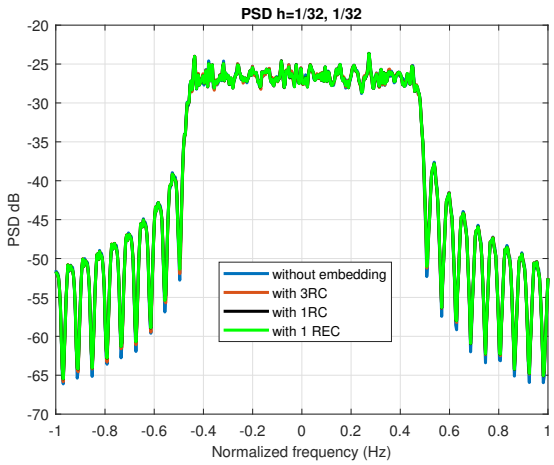

(a) PSD for h=1/32

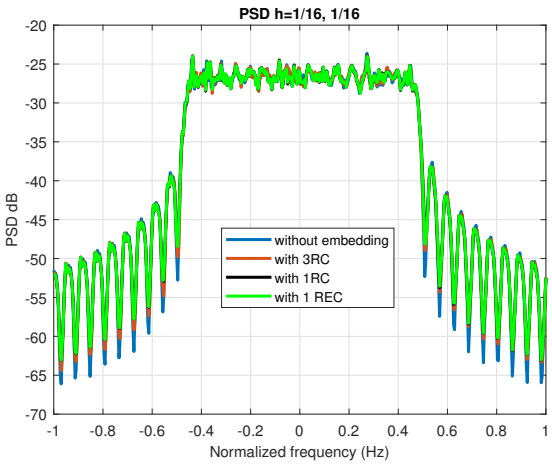

(b) PSD for h=1/16

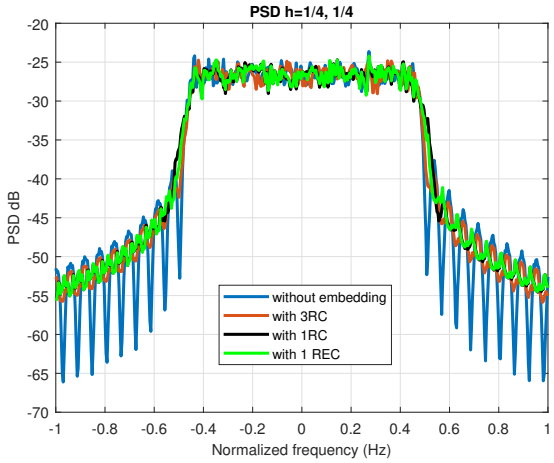

(c) PSD for h=1/4

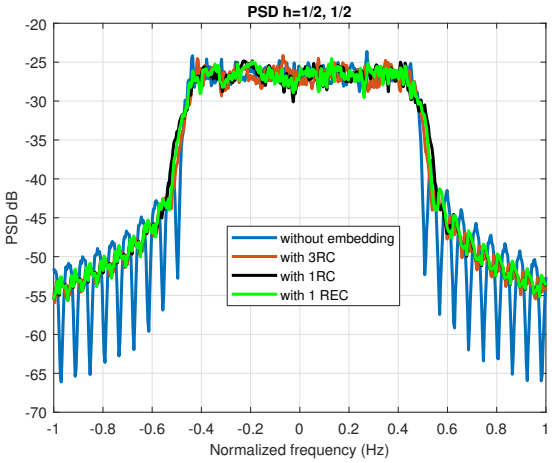

(d) PSD for h=1/2

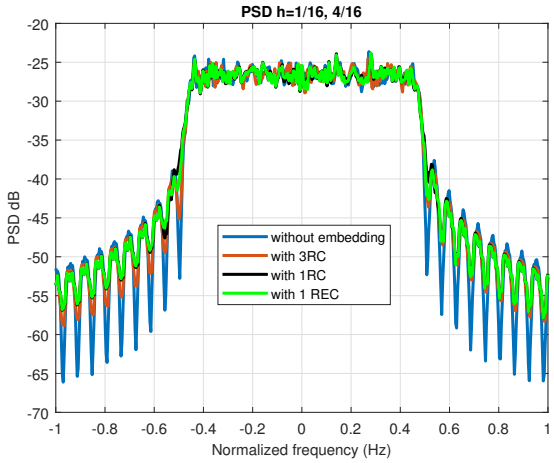

(e) PSD for $h_1 = 1/16$ and $h_2 = 4/16$

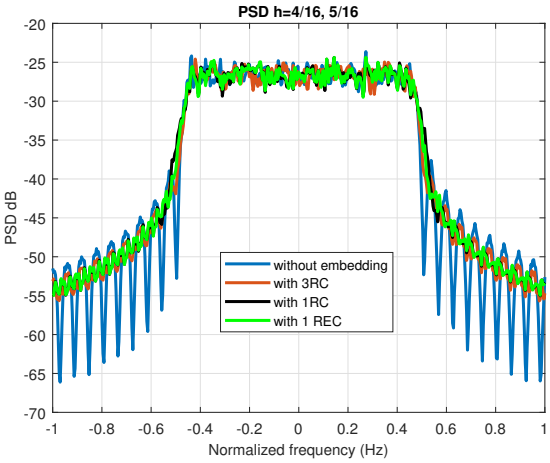

(f) PSD for $h_1 = 4/16$ and $h_2 = 5/16$

Figure 5: PSD for 4-ary CPM with different pulse shapes and modulation indices

spectral containment compared to the other two DFRC systems considered in this paper.

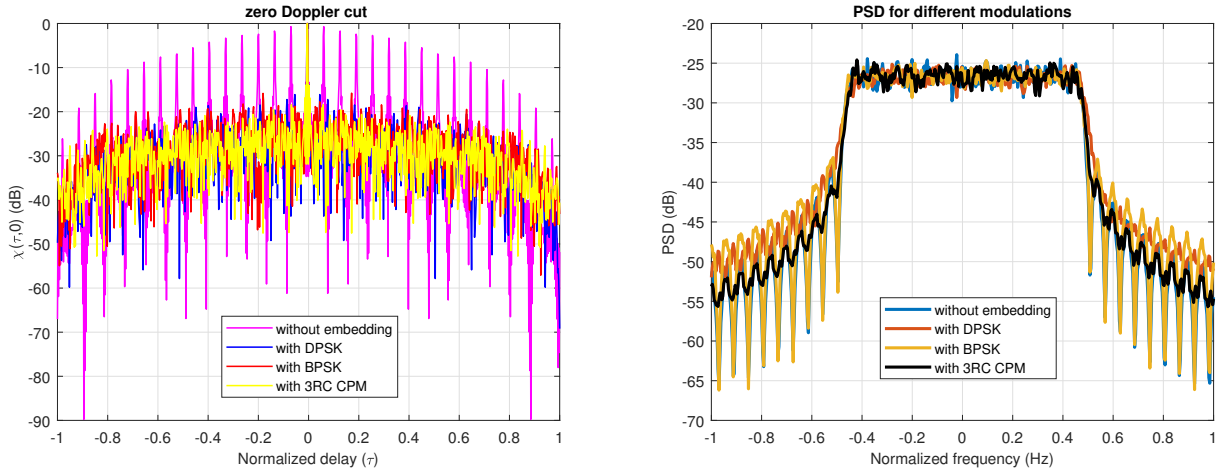

(a) RSL with and without symbol embedding (b) PSD with and without symbol embedding

Figure 6: RSL and PSD for different modulations.

6. CONCLUSION

Modulation of FH MIMO radar pulses in fast-time with DPSK and CPM modulated information symbols was presented in this paper. The RSL response and PSD of the FH/CPM and FH/DPSK DFRC systems were examined and compared with FH/PSK and FH MIMO radar system without symbol embedding. Our results showed that, the FH/CPM MIMO DFRC system has better RSL response and spectral containment compared to other FH modulated systems presented in this paper.

REFERENCES

[1] H. Griffiths, S. Blunt, L. Cohen and L. Savy, "Challenge problems in spectrum engineering and waveform diversity," in [*Proc. IEEE Radar Conf.*], 1–5 (April 2013).

[2] C. Baylis, M. Fellows, L. Cohen and R. J. Marks II, "Solving the spectrum crisis: Intelligent, reconfigurable microwave transmitter amplifiers for cognitive radar," *IEEE Microwave Magazine* **15**, 94–107 (July 2014).

[3] P. M. McCormick, S. D. Blunt and J. G. Metcalf, "Simultaneous radar and communications emissions from a common aperture, part I: Theory," in [*Proc. IEEE Radar Conf.*], 1685–1690 (May 2017).

[4] B. Li and A. Petropulu, "MIMO radar and communication spectrum sharing with clutter mitigation," in [*2016 IEEE Radar Conference (RadarConf)*], 1–6 (May 2016).

[5] J. Euzire, R. Guinvarc'h, M. Lesturgie, B. Uguen, and R. Gillard, "Dual function radar communication Time-modulated array," in [*2014 International Radar Conference*], 1–4 (Oct 2014).

[6] A. Hassanien, B. Himed and B. D. Rigling, "A dual-function MIMO radar-communications system using frequency-hopping waveforms," in [*Proc. IEEE Radar Conf.*], 1721–1725 (May 2017).

[7] S. D. Blunt and E. L. Mokole, "Overview of radar waveform diversity," *IEEE Aerospace and Electronic Systems Magazine* **31**, 2–42 (November 2016).

[8] S. Amuru, R. M. Buehrer, R. Tandon and S. Sodagari, "MIMO radar waveform design to support Spectrum Sharing," in [*MILCOM 2013 - 2013 IEEE Military Communications Conference*], 1535–1540 (Nov 2013).

[9] M. J. Nowak, Z. Zhang, Y. Qu, D. A. Dessources, M. Wicks and Z. Wu, "Co-designed radar-communication using linear frequency modulation waveform," in [*MILCOM 2016 - 2016 IEEE Military Communications Conference*], 918–923 (Nov 2016).

[10] Domenico Gaglione, Carmine Clemente, Christos V. Ilioudis, Adriano Rosario Persico, Ian K. Proudler, John J. Soraghan and Alfonso Farina, ""Waveform design for communicating radar systems using fractional Fourier transform"," *Digital Signal Processing* **80**, 57 – 69 (2018).

[11] K. Han and A. Nehorai, "Jointly optimal design for MIMO radar frequency-hopping waveforms using game theory," *IEEE Transactions on Aerospace and Electronic Systems* **52**, 809–820 (April 2016).

[12] I. P. Eedara, A. Hassanien, M. G. Amin, "Performance analysis of dual-function MIMO radar-communications using FH waveforms and PSK signalling," *IEEE Transactions on Signal Processing (submitted)* (2019).

[13] I. P. Eedara, M. G. Amin and A. Hassanien , "Analysis of communication symbol embedding in FH MIMO radar platforms," in [*Proc. IEEE Radar Conf.(accepted)*], (April 2019).

[14] C. Y. Chen and P. P. Vaidyanathan, "MIMO radar ambiguity properties and optimization using frequency-hopping waveforms," *IEEE Transactions on Signal Processing* **56**, 5926–5936 (Dec 2008).

[15] S. D. Blunt, M. R. Cook and J. Stiles, "Embedding information into radar emissions via waveform implementation," in [*2010 International Waveform Diversity and Design Conference*], 000195–000199 (Aug 2010).

[16] E. Perrins and M. Rice, "Reduced-complexity detectors for multi-h cpm in aeronautical telemetry," *IEEE Transactions on Aerospace and Electronic Systems* **43**, 286–300 (January 2007).

[17] P. Massoud Salehi and J. Proakis, [*Digital Communications*], McGraw-Hill Education (2007).

[18] I. P. Eedara, A. Hassanien, M. G. Amin and B. D. Rigling, "Ambiguity Function analysis for dual-function radar communications using PSK signaling," in [*2018 52nd Asilomar Conference on Signals, Systems, and Computers*], 900–904 (Oct 2018).

[19] H. H. Faust, B. Connolly, T. M. Firestone, R. C. Chen, B. H. Cantrell and E. L. Mokole, "A spectrally clean transmitting system for solid-state phased-array radars," in [*Proceedings of the 2004 IEEE Radar Conference (IEEE Cat. No.04CH37509)*], 140–144 (April 2004).

[20] T. Aulin, N. Rydbeck and C. Sundberg, "Continuous phase modulation - part ii: Partial response signaling," *IEEE Transactions on Communications* **29**, 210–225 (March 1981).

[21] T. Aulin and C. Sundberg, "Continuous phase modulation - part i: Full response signaling," *IEEE Transactions on Communications* **29**, 196–209 (March 1981).